

Article

A Mineralogical, Geochemical, and Geochronological Study of ‘Valencianite’ from La Valenciana Mine, Guanajuato, Mexico

Jesús Solé ^{1,*} , Teresa Pi-Puig ¹ and Amabel Ortega-Rivera ²

¹ Laboratorio Nacional de Geoquímica y Mineralogía, Instituto de Geología, Universidad Nacional Autónoma de México, Ciudad Universitaria, Coyoacán, Ciudad de México 04510, Mexico; tpuig@geologia.unam.mx

² Instituto de Geología, Universidad Nacional Autónoma de México, Estación Regional del Noroeste, Apartado Postal 1039, Hermosillo, Sonora 83000, Mexico; Dra.amabel.o.r@gmail.com

* Correspondence: jsol@geologia.unam.mx

Abstract: *Valencianite* has been described as a variety of K-feldspar (*adularia*) from La Valenciana mine, Guanajuato, Mexico, from which three samples were used for this study. We present new major and trace element analysis, X-ray powder diffraction with Rietveld refinement, and single-crystal ⁴⁰Ar/³⁹Ar ages of this classical mineral. A detailed review of major works on feldspars and relevant papers from *adularia* shows that the structure of this mineral has monoclinic and triclinic domains with variable degrees of Al/Si order that we have been only able to model by powder X-ray diffraction assuming the presence of monoclinic (~50%) plus triclinic (~50%) K-feldspar. The literature data show some extreme structural states for *adularia* obtained in the pre-Rietveld refinement era; these data are dubious and need to be reanalyzed. A triangular diagram using the relative development of {110}, {010} and {001} faces is proposed. The temperature of formation, the Na/K ratio, and the growth kinetics seem to be the main factors controlling the morphological changes in K-feldspar crystals. The geochemistry of *valencianite* shows an almost pure orthoclase composition, as is common in most *adularia* crystals, although compositions up to Or₉₀Ab₁₀ have been found. Measurement of thallium in *adularia* can be an exploration guide for ore deposits. The weighted mean of 15 ⁴⁰Ar/³⁹Ar analyses of one *valencianite* from La Valenciana mine gave an age of 30.43 ± 0.27 Ma (2 standard deviations). It is discussed whether *valencianite* can be considered a new mineral.

Keywords: alkali-feldspar; *adularia*; X-ray diffraction; Rietveld refinement; major-elements; trace-elements; Ar–Ar geochronology



check for updates

Citation: Solé, J.; Pi-Puig, T.; Ortega-Rivera, A. A Mineralogical, Geochemical, and Geochronological Study of ‘Valencianite’ from La Valenciana Mine, Guanajuato, Mexico. *Minerals* **2021**, *11*, 741. <https://doi.org/10.3390/min11070741>

Academic Editor: Alexey V. Ivanov

Received: 20 May 2021

Accepted: 2 July 2021

Published: 7 July 2021

Publisher’s Note: MDPI stays neutral with regard to jurisdictional claims in published maps and institutional affiliations.



Copyright: © 2021 by the authors. Licensee MDPI, Basel, Switzerland. This article is an open access article distributed under the terms and conditions of the Creative Commons Attribution (CC BY) license (<https://creativecommons.org/licenses/by/4.0/>).

1. Introduction

Feldspars are the most abundant minerals in the Earth’s crust, represented by the K-Na orthoclase–albite series and the Na-Ca plagioclase series. Feldspars display a simple theoretical formula XT₃O₈, where X can be Na, K, or Ca (with minor substitutions), and T is Si plus Al. Feldspars can be found in igneous, metamorphic, and sedimentary rocks, growing under wide temperature and pressure conditions. Although they have simple chemistry (predominantly consisting of the aforementioned elements), their structure is very complex and has been the subject of a myriad of works in the 20th century (see general reviews by Van der Plas [1], Smith [2,3], Ribbe [4], Brown [5], Ribbe [6], Smith and Brown [7], Parsons [8], and Deer et al. [9]). All the micro- to nanostructures observed in feldspars are produced by cooling and fluid circulation (see a review of alkaline feldspar evolution in the Klokken syenite by Parsons et al. [10]).

Although nearly all feldspars from the Earth’s crust crystallized at high (magmatic) temperatures and can be considered pseudomorphs [11], alkaline feldspars growing at low temperatures are not uncommon. They can be separated into two main groups: (a) almost pure end-member albite grown in the albitization processes (late magmatic, metamorphic, sedimentary) and (b) almost pure end-member orthoclase grown during

feldspathization processes, i.e., K-rich fluid-driven crystallization. In general, at temperatures below ~ 400 °C, either albite or orthoclase appear, rarely both. This fact is in apparent contrast to albite exsolutions in orthoclase due to unmixing of the initially homogeneous high-temperature phase sanidine due to the presence of a solvus. Sanidine is rarely preserved in plutonic rocks, although it is the primary crystallized phase. An example is the exceptionally preserved Itrongay K-feldspar from Madagascar [12,13] and some other uncommon cases. In general, sanidine is found in volcanic rocks and the rare high-temperature low-pressure sanidinite metamorphic facies.

Bambauer et al. [14] made a detailed description of the K-feldspar textures observed during the sanidine-microcline transition across metamorphic zones. This study presents descriptions and images taken with transmission electron microscopy (TEM) that elucidate the submicrometric intergrowths present at different grades of metamorphic evolution of K-feldspars. The classification of these textures prompted these authors to define the varieties sanidine, “tweed” orthoclase, irregular microcline, and regular microcline. A comparison is made [14] with the X-ray and optical varieties. Of particular importance is that these authors indicate that each K-feldspar name is dependent on the scale of observation, from low-resolution optical microscopy, through X-ray to high-resolution TEM. Bambauer et al. [14] summarizes the nomenclature that, one way or another, was used in many later works. These authors conclude that most K-feldspars, but not all, are pseudomorphs of microcline after sanidine, with complex intergrowth textures in concordance with previous work (e.g., [11]), although more detailed. TEM imaging is very compelling but is scarcely used during routine K-feldspar identification due to its complex sample preparation, interpretation, and local observational scale. X-rays have been used much more, but if applied to a mixture of states produced by cooling and fluid circulation, as is typical in plutonic rocks, can be misleading due to the average and superposed information obtained. In this case, optical observation can be a better method to discriminate the different K-feldspar textures present if TEM is not used. Powder X-ray methods can give useful information in single crystals, considering the limited resolution.

Low-temperature K-feldspar is usually called *adularia*, a word derived from the crystals of this mineral found in the Alps (Saint-Gotthard Massif, Switzerland) and described and named for the first time by Pini ([15], paragraph 145, p.115). This name is not listed as a mineral species by the International Mineralogical Association (see official list of names, IMA, 2021) because it is considered a mineral variety based on external morphology and optical properties. For practical reasons, we do not adhere in this work to the IMA rule stating that non-official mineral names or varieties must be written in italics or between quotation marks; the terms *adularia* and *valencianite* are written in plain text from now on. *Adularia* is found in many geological settings, but it is commonly unnoticed in optical microscopy and X-ray diffraction analyses due to their similarity with the more common orthoclase and sanidine (e.g., Eastwood et al. [16]). Nevertheless, many plutonic, metamorphic, and sedimentary rocks contain *adularia* crystals or overgrowths formed during cooling or diagenesis in the presence of fluids. These late feldspars have been described occasionally (e.g., [17–19]) and merits better study due to the important information they carry (age and fluid composition). The hydrothermal veins and epithermal deposits offer a different scenario. The *adularia* is present as distinctive rhomb-like crystals displaying the {110} habit, typically transparent or white, rarely confused with orthoclase, with abundant descriptions in the economic geology literature.

Among typical *adularia* stands out the *valencianite* variety found at La Valenciana mine, Guanajuato, Mexico. We report here some new data from this mineral that has been studied in very few publications. A revision of literature is summarized by 21 selected papers that are commented on in the Appendix A. We aimed to give some additional details about the structure, chemistry, and age of *valencianite* and propose a morphological classification of K-feldspars based on three prominent faces arranged in a triangular diagram. This classification is related to the temperature, the Na/K ratio, and growth

kinetics. A discussion about the possibility of naming valencianite a new mineral species is undertaken.

2. Geological Setting

Discovered by the Spaniards in the 16th century [20,21], the Guanajuato Mining District is a rich belt of silver-lead-zinc mineralization, located in the southern limit of the Mesa Central physiographic province [22], limited to the north and east by the Sierra Madre Oriental and to the south by the Trans-Mexican Volcanic Belt.

The basement in the zone comprises a thick package of Mesozoic to early Tertiary folded metamorphic rocks of marine sedimentary and volcanic origin (Esperanza Formation), intruded by dikes and stocks of late Cretaceous age and acid to intermediate composition [20,23,24].

On top of this basement, and associated with the tectonic uplift, thick units (>1400 m) of discordant and almost horizontal continental Eocene conglomerates are found [21,25–27]. These conglomerates are in turn covered by thick series (~700 m) of extrusive rocks from the late Eocene to Oligocene [22,28]. This Cenozoic volcanism has been divided into seven pulses [27], from which the felsic to intermediate Oligocene volcanism was related to the circulation of hydrothermal fluids [22,24,28] and the emplacement of the famous epithermal silver-gold mineralization of the district. The stratigraphy, tectonics, and geochronology of these rocks, denominated Guanajuato Volcanic Group (Bufa, Calderones, and Cedros formations), have been revised by Nieto-Samaniego et al. [22].

The world-class silver ore deposit was formed in a complex system of normal faults that predates and postdates the rocks of the Guanajuato Volcanic Group, mainly as veins and stockworks, but also in minor proportions as disseminations and fissure replenishments. Three NW–SE trending mineralized veins systems (La Sierra, Veta Madre, and La Luz), associated with the normal fault systems, have been distinguished (Figure 1). Several authors [21,23,29] recognized a minimum of three mineralization stages in the district (pre-ore, ore, and post-ore) and described three topographic levels of mineralization (deep ore, lower ore, and upper ore). Isotopic studies (O, C, S) suggest that the mineralization is associated with the mixing of magmatic and meteoric fluids circulated through the Mesozoic volcanic sequence. Camprubí and Albinson [30] described those deposits as epithermal with intermediate sulfidation (230 °C to 300 °C and salinities of 7.5–23 wt.% NaCl) and low-sulfidation (240 °C and salinities of 3.5–7.5 wt.% NaCl) end members. The alteration facies can be classified as argillitic, phyllic, propylitic, and potassic.

The La Valenciana mine discovered in 1771 is located at La Veta Madre (motherlode) nearby Guanajuato city. It is the most important of the three mineralized structures and one of the world's most paradigmatic epithermal silver deposits. This lode has been exploited since 1548 to date without interruption. From 1939 to the present, their exploitation is supervised by La Sociedad Cooperativa Minero Metalúrgica de Santa Fe de Guanajuato.

La Veta Madre cuts Mesozoic volcano-sedimentary rocks from La Esperanza Formation (carbon shales, calcareous lutites, and pillow andesites) covered by Oligocene volcanic rocks. Mineralization is present as veins, stockworks, disseminated, and fissure replenishments.

Paragenesis in the La Valenciana mine comprises mainly silicates (quartz-amethyst and adularia) and carbonates (calcite with different habits, dolomite, and siderite). A variable proportion of sulfides (mainly pyrite, sphalerite, and galena) were also described [23]. Acanthite, aguilarite, and naumannite are essential silver-bearing minerals. Gold occurs in the native state and as electrum. The detailed mineralogy was described by Petruck and Owens [31] and Moncada et al. [24,32], among other authors.

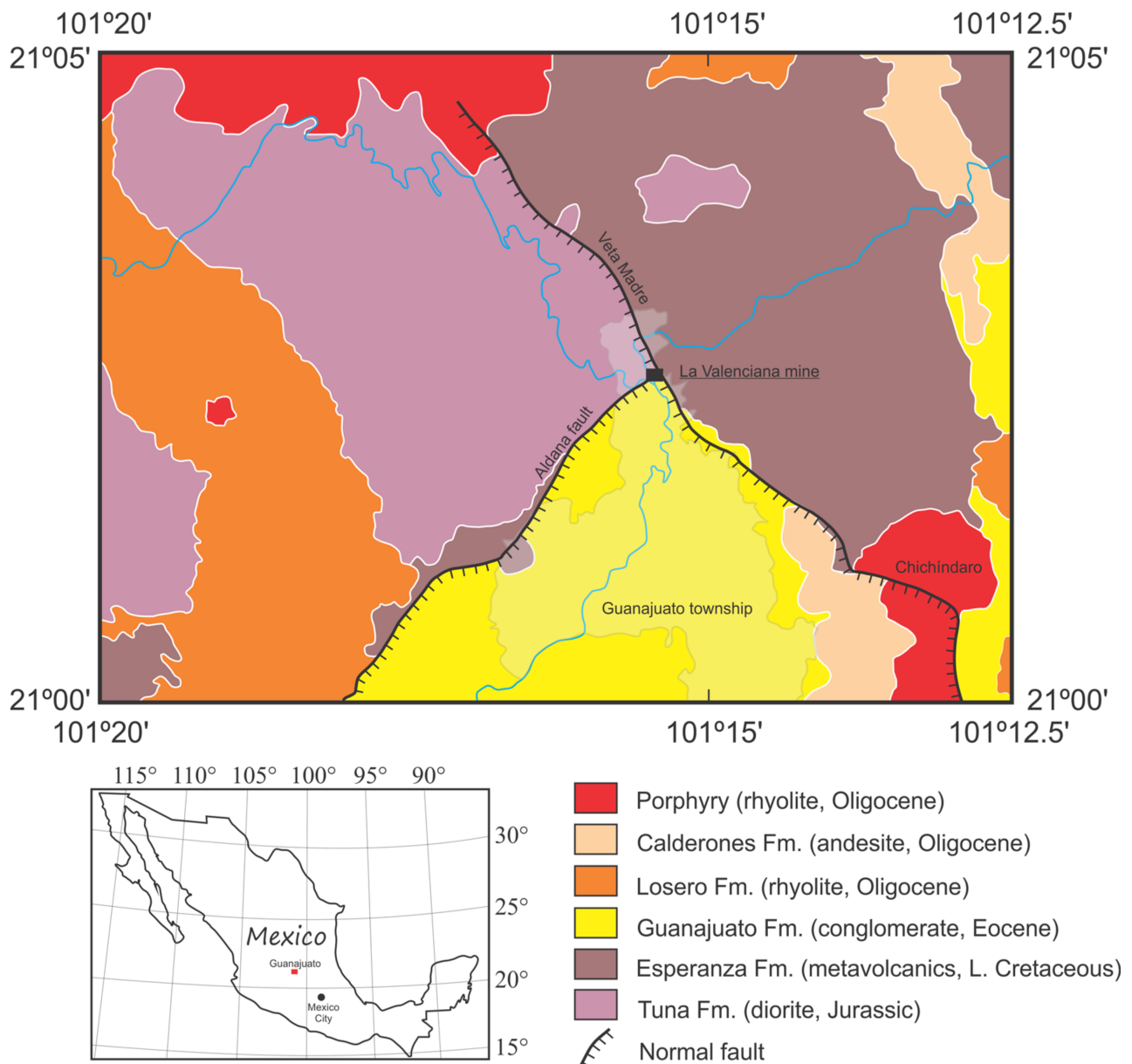


Figure 1. Geological map of the Guanajuato region showing the location of La Veta Madre and La Valenciana mine. Simplified from the Mexican Geological Survey cartography (Servicio Geológico Mexicano, <https://www.gob.mx/sgm> (accessed on 10 March 2021)).

Valencianite is found as relatively large crystals developed above a brecciated quartz matrix. There are reports of valencianite from other nearby mines, like La Sirena and Caliche. This mineral was named “chovelia” (in honor of Mr. Casimiro Chovell, administrator of La Valenciana) by del Río [33] after it was described by Humboldt [34], who identified this mineral as an orthoclase variety. Del Río [33] described this mineral as similar to adularia but with curved faces and higher hardness.

3. Samples and Methods

Three samples from the La Valenciana mine have been studied (Figure 2). Valencianite crystals come out in dense associations, forming crusts with some quartz. Crystal size is about 2–3 cm for sample #1 and from several mm to 1 cm in samples #2 and #3. Samples #2 and #3 were cut to make a thin section for optical observation. Several crystals of each sample were isolated mechanically and ground in a steel mill. The resultant powder was

studied by X-ray diffraction, X-ray fluorescence, and inductively coupled plasma mass spectrometry (ICP-MS).

X-ray diffraction analyses were obtained with a Shimadzu XRD-6000 powder diffractometer (Shimadzu Corporation, Kyoto, Japan) equipped with a Cu tube and graphite monochromator. The configuration of the diffractometer is presented in Table 1.



Figure 2. Valencianite hand samples studied in this work. All specimens from the La Valenciana mine, Guanajuato, Mexico.

Table 1. Technical data for the X-ray diffractometer used for the Rietveld refinement.

Parameter	Value
X-ray diffractometer	Shimadzu XRD-6000
Geometry	Bragg-Brentano
Goniometer radius	185 mm
Radiation source	CuK α
Generator	40 kV, 30 mA
Tube	Fine focus
Divergence slit	$\frac{1}{2}^\circ$
Receiving slit	1°
Soller slits	5.729° (0.10 rad)
Resolving slit	0.15 mm
Monochromator	Graphite (diffracted beam)
Detector	Scintillation counter
Step size	0.02°
Integration time	4 s

The X-ray diffraction data have been analyzed with the Rietveld method [35] using TOPAS Academic software (version 4.1, Coelho Software, Brisbane, Australia). This software implements the fundamental parameters approach [36]. The specimen-dependent parameters which were refined were zero error, displacement error, Chebyshev polynomial fitting for the background with eight coefficients, cell parameters, crystallite size, microstrain, and preferred orientation with spherical harmonics.

Chemical analyses of major elements from the three valencianite samples were undertaken on a SRS-3000 X-ray fluorescence spectrometer (Bruker, Karlsruhe, Germany), calibrated against international reference materials [37]. Trace elements were measured on valencianite sample #1 by ICP-MS using alkaline fusion and subsequent dissolution (Actlabs Laboratories, Ancaster, ON, Canada).

Geochronological data on single-crystal fragments of valencianite were compiled using the Ar-Ar technique. Crystals were separated from sample #1. These crystal fragments

were concentrated by standard techniques and later selected by handpicking under a binocular microscope from fractions that ranged in size from 400 μm to 250 μm at the mineral separation laboratory at Estación Regional del Noroeste, Instituto de Geología, Universidad Nacional Autónoma de México (Hermosillo, Sonora). Mineral separates were loaded into Al-foil packets and irradiated at the McMaster Nuclear Reactor (Hamilton, ON, Canada). $^{40}\text{Ar}/^{39}\text{Ar}$ analyses were performed by standard laser step heating techniques described in detail by Clark et al. [38] at the Geochronology Research Laboratory of Queen's University (Kingston, ON, Canada). All data were corrected for blanks, mass discrimination, and neutron-induced interferences.

4. Results and Discussion

4.1. Morphology

The valencianite from the type locality is found to be plates forming the wall of veins that display a base (the outer part of the vein) of quartz plus feldspar, and an internal part formed up mainly by the euhedral valencianite plus minor quartz and some accessory minerals like siderite (Figure 2). The stepped nature and curvature of some faces are noteworthy in the largest crystal from sample #1.

The atlas of crystalline forms (vol. III) from Goldschmidt [39] displays 46 drawings of adularia crystals published from 1828 to 1902. The {110} tracht is prominent in adularia. A detailed inspection of the La Valenciana hand samples (combined with the crystal morphology observed in the thin sections) shows that almost all crystals have the aforementioned morphology. In these hand samples (Figure 2), the genetic features listed by Černý and Chapman ([40], p.725–726) cannot be used as a classification scheme because valencianite presents crystals of Felsöbanya–Maderaner habit but have a very coarse size and crystals are not transparent, but white. Nevertheless, the genetic explanations proposed by these authors [40] are coincident with our observations and the ternary diagram presented below.

Combining the observations from the literature described in the historical background section (see Appendix A), the figures reported by Goldschmidt [39], and the books on feldspars cited in the introduction, we concluded that the three most essential faces that define the habit of K-feldspars are {110}, {010}, {001}, followed by $\{-101\}$ and $\{-201\}$. This observation coincides with the results of Franke and Ghobarkar [41] and Woensdregt [42]. Taking only the first three prominent faces, we made a triangular diagram (Figure 3). A square diagram with these faces plus $\{-101\}$ is also possible, but we have not attempted it due to the lack of comprehension of all variables. This new diagram has been interpreted as having two correlative variables, temperature and Na/K ratio, that increase following the development of {010} and running from {110} and {001}, respectively. The development of {001} vs. {110} and {010} is probably related to the kinetics of crystallization, as shown in the diagram. This ternary plot is coherent with the phase diagram of alkali feldspars and the increased proportion of albite in orthoclase up to approximately $\text{Ab}_{0.5}\text{Or}_{0.5}$ at higher formation temperatures. More studies must be undertaken to fully understand these variables and their correlation with the external morphology of alkali feldspars.

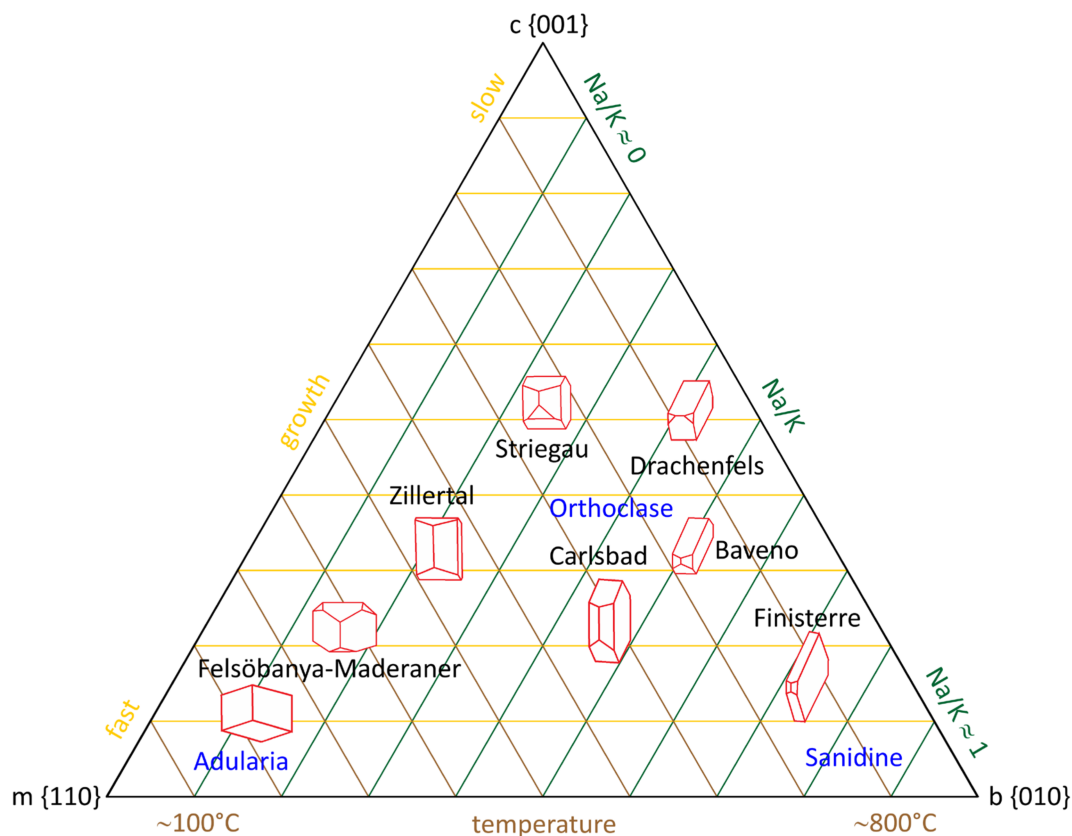


Figure 3. Triangular diagram showing the relative development of crystal faces of alkali feldspars. The significance of the scales is hypothetical, based on face development observations in different feldspars and bibliographical information (see text). Some crystal tracht names after [43].

Nevertheless, some correlations between face development with temperature, kinetics, chemistry, maybe pressure must be explored further. It must be noted that most feldspars are anhedral due to their growth being limited by adjacent crystals, so their external morphology is seldom visible. Smith ([3], p.256) presents some graphs from previous authors about the relative development of faces and makes a detailed review and discussion of the trach, habit, and morphology in chapter 17.3 of his book. It is known but not well understood that crystal morphology is dependent on their chemical-physical conditions of formation, an issue demonstrated well by Pupin [44] in the zircon case and by other authors in some minerals like quartz, pyrite, and calcite [45,46]. The characteristic habit of adularia is related to their mode of occurrence: low-temperature veins and hydrothermal replacements with a low Na/K ratio.

4.2. Optics

A cut of the two samples with intermediate dimension crystals (samples #2 and #3) was made, and a polished thin section was made from both. A microscopic, polarized image of two sections was obtained using a mosaic of photographs (Figure 4). It is evident in the images that adularia crystals are not homogeneous, showing several extinction directions in almost every crystal. In the available literature, sections were typically taken perpendicular to c in order to display better the orientation of the optical axes plane and $2V$ angle, a study that has been performed in several works already mentioned above. Our sections were cut parallel to the c axis, which better shows the growing morphology of crystals. All faces grew as sectors that gave the polygonal nature of grey shades in the images. It is so evident that some crystals have a tridimensional appearance in the photograph from the polished section. These are the crystal faces discussed in the literature that show variable optical orientations. Face curvature is also displayed in some crystals.

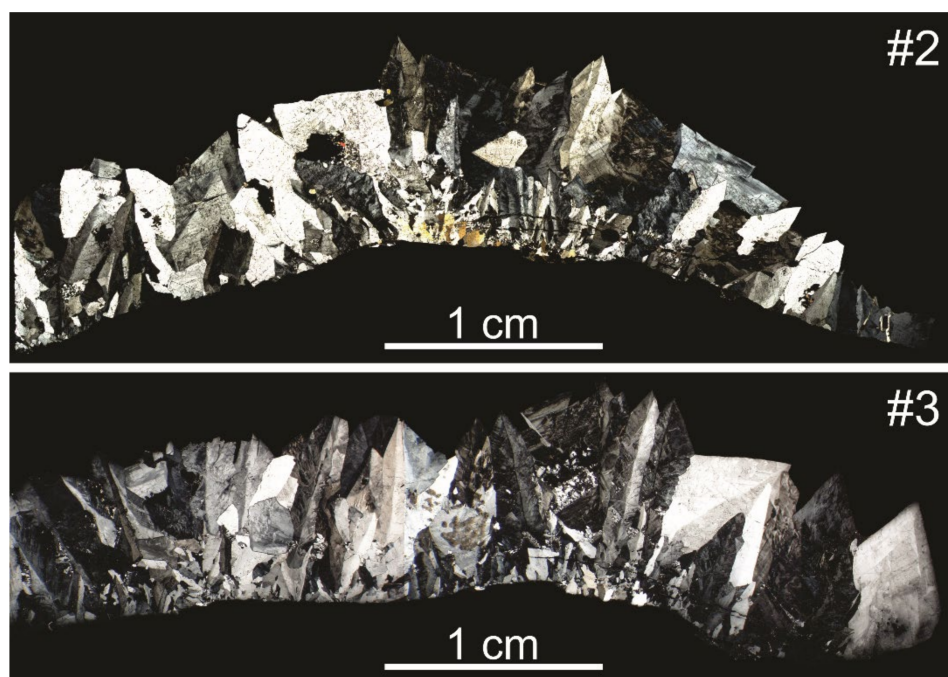


Figure 4. Photomicrographs of valencianite samples #2 and #3 (Figure 2) showing diverse textures in thin sections. The figure is a mosaic of photographs made with an AxioImager A2.m microscope using crossed polarizers and a $\times 2.5$ objective.

4.3. Crystal Structure and Al-Si Ordering

Samples #1 and #3 (large and medium crystals) were measured by X-ray diffraction and refined with the Rietveld method. The refinement results are summarized in Table 2. Our X-ray analysis by the Rietveld method shows that a good fit of the full profile can only be obtained if two phases, microcline, and sanidine, are mixed (Figure 5). A single monoclinic or triclinic phase cannot account entirely for the peaks observed in the diffractogram. Optical microscopic observation shows (Figure 4) that valencianite is not homogeneous, and various textures appear. Some crystals have sector growth, undulate extinction, and twins, but others are entirely homogeneous. These facts explain why cell refinements of these mixtures by classical indexing techniques are not reliable.

Table 2. Cell parameters for sanidine and microcline phases obtained in the Rietveld refinement of adularia from La Valenciana mine, Guanajuato, Mexico.

Parameters	Valencianite #1		Valencianite #3	
	Rwp = 4.26; Gof = 1.25		Rwp = 4.94; Gof = 1.40	
	Sanidine	Microcline	Sanidine	Microcline
<i>a</i>	8.5950 (14) *	8.5967 (13)	8.5969 (17)	8.5959 (17)
<i>b</i>	13.0110 (20)	13.0289 (20)	13.0103 (26)	13.0338 (26)
<i>c</i>	7.1866 (11)	7.1734 (11)	7.1907 (15)	7.1751 (14)
α	90.0°	90.0802° (41)	90.0°	90.0775° (52)
β	116.0627° (34)	116.0727° (32)	116.0454° (32)	116.0479° (47)
γ	90.0°	89.6739° (41)	90.0°	89.6680° (52)
<i>a</i> *	0.12952	0.12950	0.12958	0.12956
<i>b</i> *	0.07686	0.07675	0.07690	0.07680
<i>c</i> *	0.15490	0.15520	0.15496	0.15524
α^*	90.0°	90.0703°	90.0°	90.0700°
β^*	63.9373°	63.9274°	63.9558°	63.9440°
γ^*	90.0°	90.3238°	90.0°	90.3023°
<i>V</i>	721.96 (20)	721.68 (19)	722.58 (25)	722.21 (25)

Table 2. Cont.

Parameters	Valencianite #1		Valencianite #3	
	Rwp = 4.26; Gof = 1.25		Rwp = 4.94; Gof = 1.40	
	Sanidine	Microcline	Sanidine	Microcline
density	2.56345 (71)	2.56442 (69)	2.56123 (89)	2.56256 (89)
X _{Or}	0.96	0.96	0.98	0.97
% phase	41.3 (2.2)	56.8 (2.2)	57.8 (2.0)	41.8 (2.0)

* One standard deviation in the last digits. % phase is the percentage of each structure in each sample; includes 1.9% quartz in valencianite #1 and 0.4% quartz in valencianite #3. Rwp: weighted profile R-factor. Gof: goodness of fit.

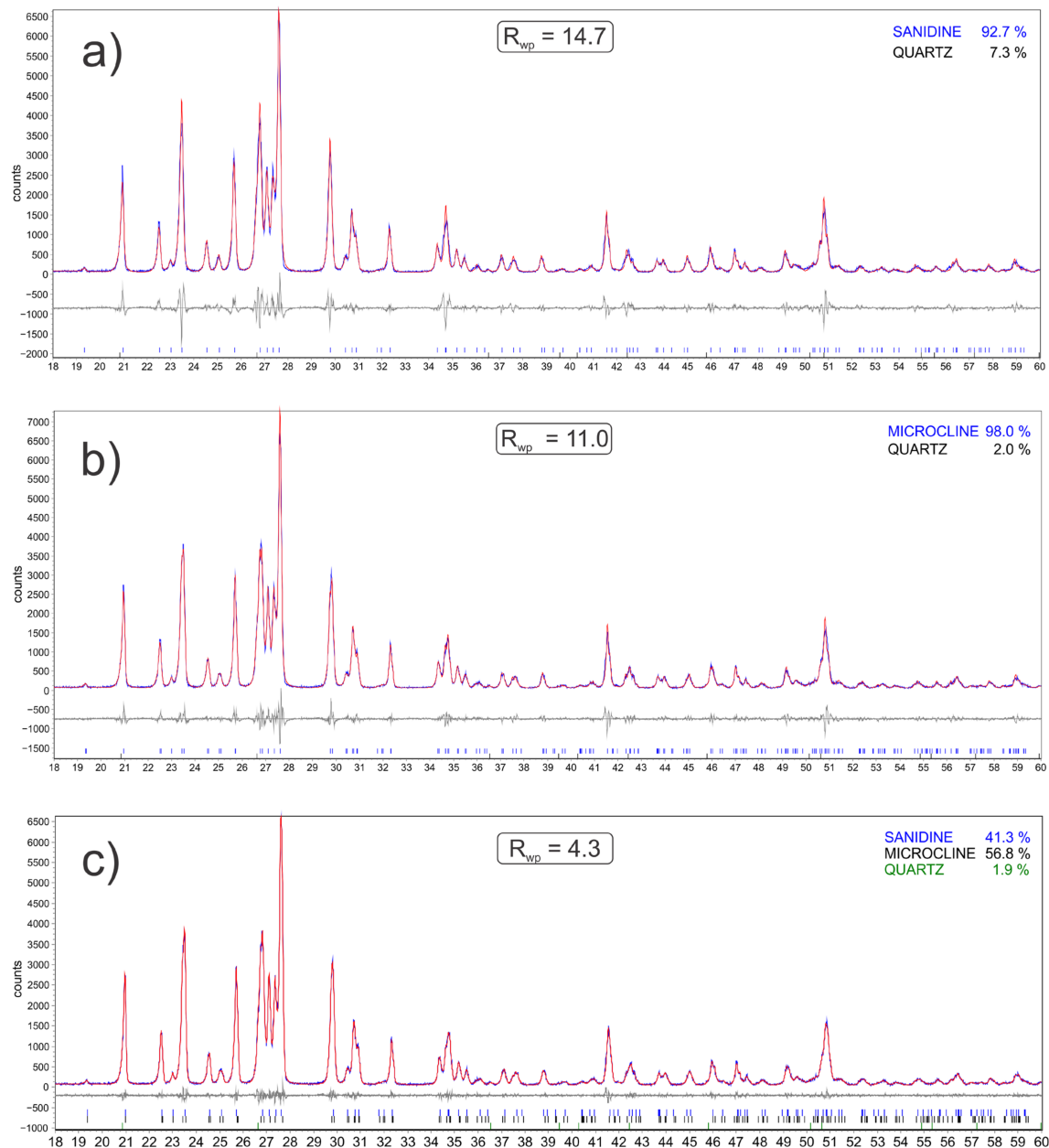


Figure 5. Rietveld refinement of adularia sample number #1 from the La Valenciana Mine, Guanajuato, Mexico. Three refinements were done to show the quality of fit using different assumptions about the crystal structure of valencianite: (a) (top) monoclinic sanidine symmetry (+quartz); (b) (middle) triclinic microcline (+quartz); and (c) (bottom) a mixture of monoclinic plus triclinic structures (+quartz). Results reported in Table 2 are based on the (c) refinement.

Feldspars show a superposition of peaks, some by lack of resolution, and others because the crossing of hkl reflections derived from different structural states can invert reflections' order [13]. It is challenging to choose the right hkl for specific reflections by hand. Only the Rietveld method can extract useful information even in the case of severe peak overlap. Our results show that valencianite is in the right corner of the *b-c* parallelogram, i.e., near the microcline-sanidine join (Figure 6). Observe that only two of the published valencianite from La Valenciana mine are near our results (one sample from Černý and Chapman [40], and the other from Sánchez Muñoz et al. [47]) while cell parameters from Taylor [19] are very dispersed, like many measurements of adularia shown in Figure 6 (far from the high sanidine—maximum microcline join). This fact has been taken as proof of the 'extremes' of the structural state of adularia s.l. [40]. We think that most of these data are questionable for the abovementioned reasons. Indexation of peaks by hand is not advised for feldspars with a mixture of structural states. Černý and Chapman ([40], p.724) admit that the 'extreme' structural states of adularia found by them can be a fictitious: "... result from shifts induced into the monoclinic diffraction-maxima by overlaps with the triclinic peak aggregates". The cell dimensions obtained by us are averages of a probably extensive range of structures, from which two predominates, sanidine (ordered) and microcline (disordered) (Table 2), and is also common in K-feldspars from slowly cooled plutonic rocks. Although this was recognized in adularia long ago, it was not expected for a low-temperature feldspar.

If the works of Chaisson [48], Akizuki and Sunagawa [49], and Černý and Chapman [40] are combined, together with some conclusions from other works cited in the Appendix A, one can hypothesize that crystallization at relatively high temperature gives ordered monoclinic adularia, and progressive temperature decrease during crystal growth will finally give disordered triclinic adularia. This sequence is contrary to the classical knowledge of magmatic feldspars, which display disordered Al/Si distribution in the high-temperature monoclinic sanidine and ordered Al/Si in the low-temperature microcline, i.e., cooling promotes Al/Si ordering. Therefore, adularia must be a metastable phase, as indirectly suggested by Bambauer and Laves [50]. A plausible explanation for their formation must be linked to kinetic factors, not thermodynamic ones. Hovis [51] devised a diagram for determining the temperature of formation of alkali feldspars based on crystallographic parameters, but it fails for adularia and valencianite. Therefore, Al/Si ordering and related parameters cannot be used for such a purpose in this type of feldspar.

Summarizing all the above literature and discussion, we can hypothesize a double route for the observed Al/Si ordering and structure of adularia. First, a hydrothermal path of fast crystallization from a moderately hot fluid (150–300 °C, maybe up to 400 °C), associated with epithermal deposits and alpine-type veins. This adularia can grow during ebullition, grossly favoring kinetic effects. It is mainly monoclinic and ordered but develops triclinic domains controlled by kinetics. Second, adularia crystallize as overgrowths or replacements, occasionally single crystals, which grow late and slowly in many intrusive and metamorphic rocks, whose presence is in general unnoticed. In this case, the adularia structure is controlled mainly by the fluid temperature that produces the replacement and growth, gradually evolving by cooling or eventual annealing to a triclinic (microcline) phase.

4.4. Chemistry

Major element analyses are shown in Table 3. It is noteworthy that many studied adularia in the literature, irrespective of their ambient formation, is almost pure K feldspar, incorporating few Na and negligible Ca, although compositions up to Or₉₀Arb₁₀ have been reported. Thus, during its low-temperature and low-pressure formation, the availability of the K⁺ cation must have been higher than Na⁺ in the fluid phase, or albite would have formed instead.

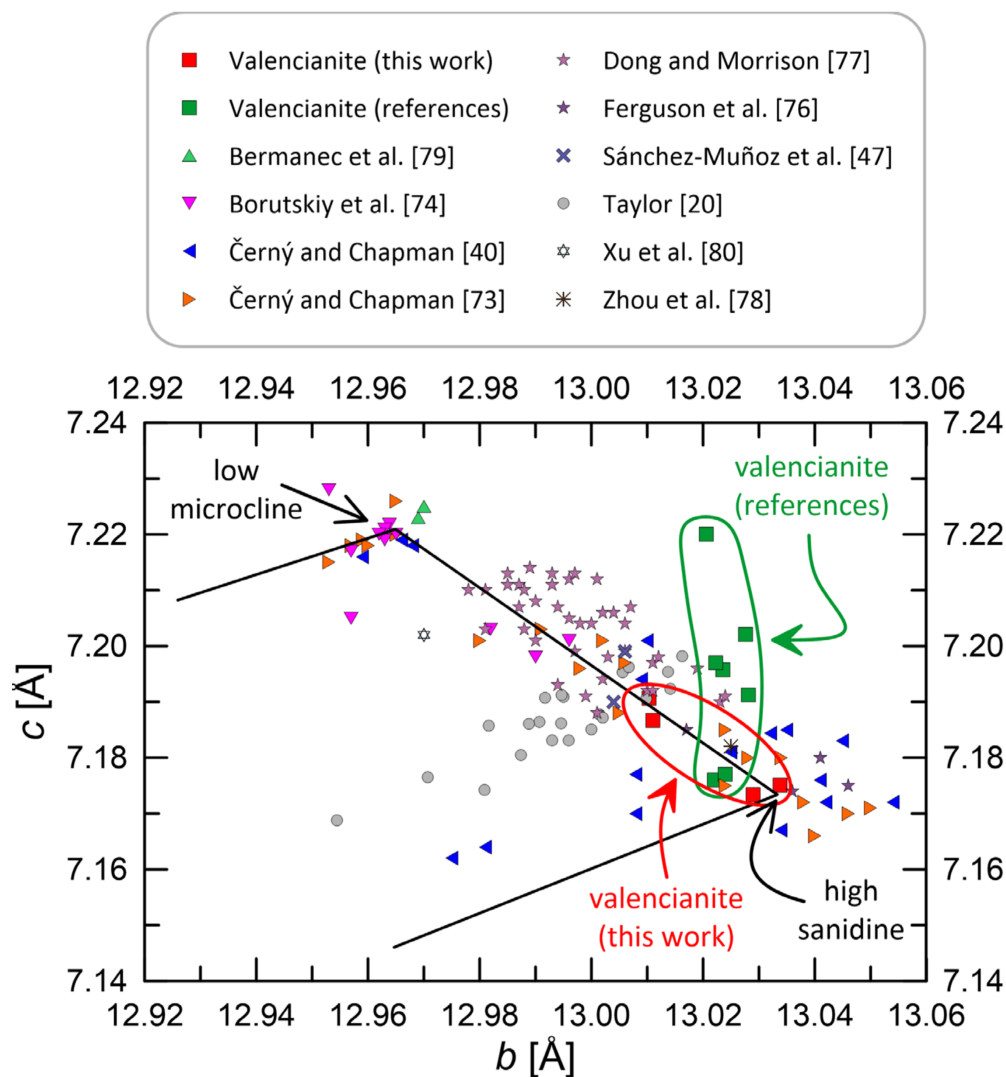


Figure 6. A *b-c* plot [52] from valencianite and adularia, including data from this work and bibliography. Black lines are the joints connecting the alkali feldspars series.

Trace elements are presented in Table 4. In the case of valencianite, many trace elements were not detected at all, and from the list of those that were, only Rb, Sr, and Ba show a remarkable concentration. Rubidium and barium are easily understood in the K-feldspar structure. The 0.28% of BaO and 0.11% of Rb₂O are not unusual concentrations for orthoclase. Strontium at 50 ppm is also a normal concentration for an almost pure K feldspar, with very few Ca substitution.

Table 3. Major element composition and structural formula of adularia samples 1, 2, and 3 (this work), Guanajuato adularia ([40], Table 1), and adularia Spencer E [53].

Oxide	#1	#2	#3	Guanajuato	Spencer E
SiO ₂	66.32	65.33	65.50	64.90	64.28
TiO ₂	0.01	0.01	0.01	-	-
Al ₂ O ₃	17.47	17.81	17.87	18.20	19.19
Fe ₂ O ₃	0.07	0.08	0.09	-	0.09
MgO	0.10	0.10	0.15	-	0.10
CaO	0.01	0.01	0.02	-	0.11
BaO	0.28 *	-	-	-	0.11
Na ₂ O	0.28	0.23	0.26	-	0.92

Table 3. *Cont.*

Oxide	#1	#2	#3	Guanajuato	Spencer E
K ₂ O	15.58	16.03	15.85	16.50	15.30
P ₂ O ₅	0.02	0.01	0.03	-	-
L.O.I.	-	-	0.29	-	0.36
Total	100.14	99.61	100.06	99.60	100.35
Atoms (8 oxygens)					
Si	3.049	3.024	3.023	3.010	2.964
Ti	0.000	0.000	0.000	0.000	0.000
Al	0.947	0.971	0.972	0.995	1.043
Fe	0.002	0.003	0.003	0.000	0.003
Mg	0.007	0.007	0.010	0.000	0.007
Ca	0.001	0.001	0.001	0.000	0.005
Na	0.025	0.021	0.023	0.000	0.082
K	0.914	0.947	0.934	0.976	0.900
P	0.000	0.000	0.000	0.000	0.000
Total	4.945	4.973	4.967	4.981	5.004

^ not determined. * calculated from trace elements (Table 4). L.O.I.: Loss on ignition.

Table 4. Trace elements from adularia sample #1 from La Valenciana mine, Guanajuato, Mexico. All elements in $\mu\text{g}\cdot\text{g}^{-1}$.

Not Detected				Detected			
V	<5	In	<0.1	Ga	7	Nd	0.45
Cr	<20	Eu	<0.005	Rb	1060	Sm	0.15
Co	<1	Ho	<0.01	Sr	50	Gd	0.13
Ni	<20	Tm	<0.005	Zr	6	Tb	0.01
Cu	<10	Lu	<0.002	Nb	5.8	Dy	0.05
Zn	<30	Ta	<0.01	Sn	1	Er	0.02
Ge	<0.5	W	<0.5	Sb	0.6	Yb	0.02
As	<5	Pb	<5	Cs	15.0	Hf	0.1
Y	<5	Bi	<0.1	Ba	2550	Tl	12.80
Mo	<2	-	-	La	0.42	Th	0.27
Ag	<0.5	-	-	Ce	0.98	U	0.13
-	-	-	-	Pr	0.11	-	-

A more remarkable fact is thallium (12.8 ppm) at higher levels than the concentration of this element in the crust (0.9 ppm), which is not completely surprising because most of the production of thallium derives from the smelting of lead-zinc ores, and the La Valenciana mine is one of such base-metal mines (including silver). Thallium is concentrated in feldspars and micas and the ore-forming minerals galena and sphalerite [54–56]. Nevertheless, the concentration of Tl in valencianite is relatively high for feldspar from a non-alkaline rock, which is an issue that requires more close inspection in a range of feldspars from diverse geological settings by virtue of the possible ore exploration interest.

4.5. Age

Table 5 shows the ages obtained with the Ar–Ar method in 15 single crystal fragments. There were four ages already published from valencianite [20–22,57]. All these ages plus the Ar–Ar obtained in this work are presented in Figure 7. From all these data, it can be concluded that mineralization at La Veta Madre, Guanajuato, must have occurred between 30 Ma and 27 Ma, but the age of adularia itself is worth discussion. Taylor [20] and Gross [21] ages on adularia were obtained with the K–Ar method. Taylor [20] cites, in his Ph.D. thesis, an age of 27.4 Ma for a sample of adularia from Veta Madre, that this author sends to P. E. Damon (Tucson, Arizona) for dating in 1971. No complementary analytical data were given. This date has been erroneously cited by [57] as having an error of 4 Ma, but [20] states (two times) “27.4 ± 4 Myr” that we interpret as 0.4 Ma, which is more in accordance with the typical error of the K–Ar laboratory of Paul Damon,

as observed in several of his publications (about 2%, one standard deviation). This age must be recalculated using the Steiger and Jäger [58] constants ($27.4 \times 1.0262 = 28.1$ Ma). Gross [21] cites the existence of four dates of adularia from Veta Madre that range from 27.4 ± 0.4 to 29.2 ± 2.0 Ma. No more information is given. It is almost certain that the former of these dates is that of Taylor [20]. We have not found the original references (besides the aforementioned coincidence), so we cannot do more than recalculate the oldest age of 29.2 to the new value (30.0 Ma, see Figure 7).

Table 5. Total fusion ages of 15 crystal fragments from adularia sample #1 from la Valenciana mine, Guanajuato, Mexico.

Experiment	Age (Ma)	$\pm 1sd$	% ⁴⁰ Ar	Ca/K	Experiment	Age (Ma)	$\pm 1sd$	% ⁴⁰ Ar	Ca/K
1	30.24	0.32	21.46	0.024	3	30.23	0.39	23.60	0.034
1	30.89	0.99	45.35	0.002	3	30.42	0.33	28.28	0.010
1	30.41	0.67	24.96	0.002	3	30.89	0.57	42.81	0.015
1	30.41	1.31	38.04	0.008	3	30.46	0.5	23.53	0.013
2	30.09	0.28	17.77	0.540	3	30.69	0.26	16.01	0.000
2	30.37	0.54	19.04	0.003	3	31.06	0.89	17.63	0.005
2	30.37	1.42	38.48	0.001	3	30.79	0.8	20.36	0.000
-	-	-	-	-	3	30.87	0.82	42.38	0.008

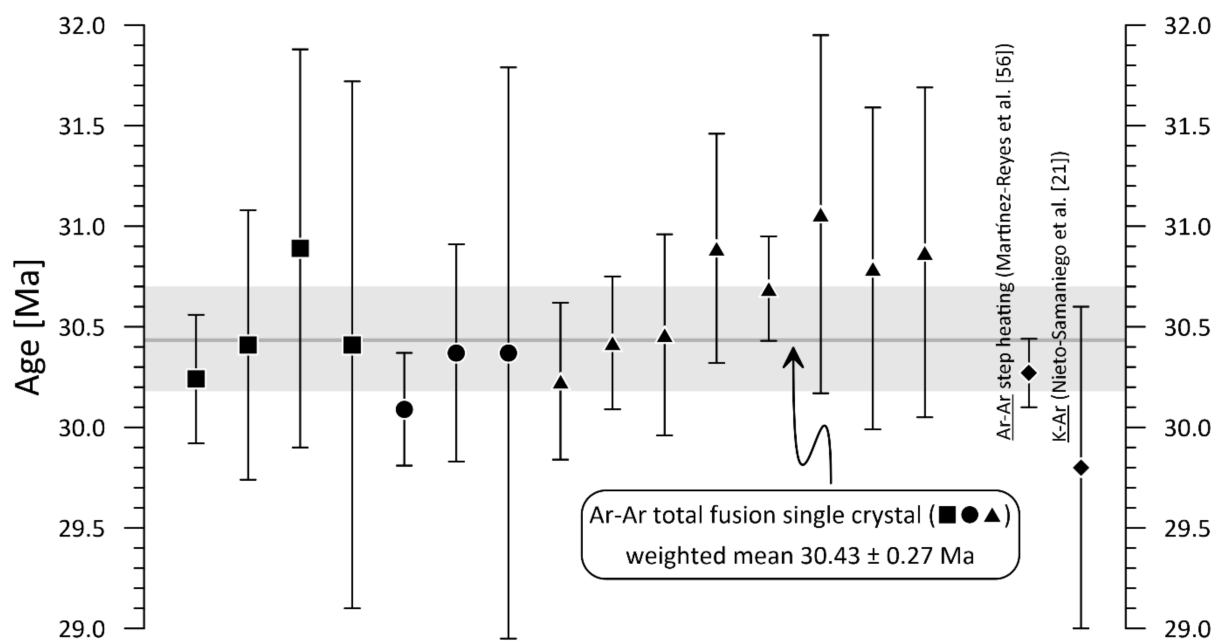


Figure 7. A plot of available Ar–Ar and K–Ar ages from valencianite (La Valenciana, Guanajuato, Mexico). The symbols square, circle, and triangle correspond to experiments 1, 2, and 3 from Table 5. Error bars are one standard deviation.

A detailed observation of Table 5 and Figure 7 shows that the age of valencianite is not as “unique” as one can think. K–Ar ages of feldspar can be lower than the true age owing to the lack of complete argon extraction due to the high viscosity of the melt, a well-known problem. Therefore, K–Ar ages on hydrothermal feldspars using classical techniques can be low, rarely high. Ar–Ar dating does not suffer from this limitation because samples do not need to be wholly fused nor argon completely extracted to give an age. Martínez-Reyes et al. [57] obtain a plateau age of 30.20 ± 0.17 Ma from a step heating Ar–Ar experiment. Their total integrated age is similar, at 30.27 Ma. The same work indicates a Rb–Sr age of 28.47 ± 0.55 Ma (28.93 Ma with the new ⁸⁷Rb decay constant, [59]) for the illite from a nearby ore, which represents probably the last stage of mineralization in the area. Our single crystal Ar–Ar ages show a weighted mean of 30.43 ± 0.27 Ma. Within errors, step heating Ar–Ar and single-crystal ages are indistinguishable. The K–Ar age of

29.8 ± 0.8 Ma of Nieto-Samaniego et al. [22] is also equivalent. With the published data, including this work, it is impossible to ascertain if only one adularia crystallization event exists or that this mineral has grown in continuous or discrete events between ~ 29.5 and ~ 30.5 Ma, although the most probable is a crystallization event at 30.4 ± 0.3 Ma.

4.6. The Mineral ‘Variety’ Problem. Is Valencianite a New Mineral?

Valencianite is considered a synonym or a variety of adularia. Vander Plas ([1], p.1,25) defines adularia as ‘modifications of feldspars rich in potassium’ along with orthoclase, sanidine, and microcline, i.e., a mineral species, using current terminology. Smith ([2], p.14) states, ‘it should be mentioned that the terms adularia, pericline and cleavelandite should be reserved for habits of feldspars and not for specific structural properties,’ i.e., not a mineral species, although this sentence is ambiguous. Smith and Brown ([7], Ch.9) seem to contradict Smith [2] in their doubt about defining adularia as a true mineral species like orthoclase or microcline. It seems that if orthoclase is a mineral, being a mixture of triclinic domains, so it will be adularia. A curious note, apparently not completely explored today, is that Smith and Brown ([7], p.28) discuss that all feldspars seem to be strictly centrosymmetric, except adularia, which can display a pyroelectric effect ([2], p.39).

In many papers adularia is defined as a ‘K-feldspar variety.’ This definition is problematic because the term ‘variety’ can only be assigned to a mineral species, not to a superior level like ‘K-feldspar’ due to the taxonomical mineralogical classification (e.g., [60]). The sublevels of ‘K-feldspar’ are the mineral species, and the ‘variety’ can only apply to a concrete mineral species. In other words, is adularia a ‘variety’ of sanidine, orthoclase, or microcline? That is the main problem of the use of the ‘variety’ word in taxonomical classification. The classification of K-feldspars infringes the basic rules [60].

Adularia or valencianite have been postulated as a new mineral species in at least three publications: Chaisson [48], Gubser and Laves [61], and Sánchez-Muñoz et al. [47]. The first two state that adularia shares the optical and structural properties of sanidine, microcline, and orthoclase in an apparently inconsistent way. The latter author defines feldspar mineral species from medium-range ordering schemes with specific atomic arrangements for local charge compensation, from data obtained by nuclear magnetic resonance spectroscopy, indicating that valencianite and sanidine have different structural states. A recent work [62] proposes a new definition of ‘mineral species.’ If we follow the definition given by these authors, a mineral species must have a particular end-member formula, space group, Z, and bond topology. Adularia or valencianite do not have a different end-member formula than orthoclase; do not have a different space group than sanidine or microcline, and they have apparently the same Z and similar sanidine bond topology. These data suggest that adularia or valencianite cannot be a new mineral. However, the same problem can be applied to orthoclase when compared to sanidine and microcline. Our many tries with the Rietveld refinement of valencianite and the impossibility of refining the structure satisfactorily without using monoclinic plus triclinic structures in a K-feldspar that has not cooled slowly from high temperatures suggests that the topological issue is not completely solved and that valencianite or adularia are composed by both sanidine and microcline structural states. A typical dominant {110} morphology with curved edges and faces plus all the above characteristics and singularities indicate that the creation of an adularia or valencianite ‘mineral species’ remains an open question. However, the authors are more inclined to think that valencianite or adularia, as found in the La Valenciana mine and based on our Rietveld refinements in the X-ray diffraction patterns, is a mineral species due to the unfortunate use of the term ‘variety’ in the alkali feldspar ‘subgroup,’

5. Conclusions

Valencianite, a ‘variety’ of K-feldspar from the La Valenciana mine, Guanajuato (Mexico), is a characteristic mineral with compositional similarities to other adularia but somewhat different by the presence of a particular structural state.

Valencianite shows a structure that we modeled with sanidine (~50%) plus microcline (~50%). The simultaneous presence of various structures makes manual indexing for cell parameter refinement doubtful. The literature data of adularia that shows extreme structural states could have been miscalculated because it was obtained before the Rietveld method was well established for X-ray diffraction.

The weighted mean of 15 $^{40}\text{Ar}/^{39}\text{Ar}$ analyses of one valencianite from La Valenciana mine gave an age of 30.43 ± 0.27 Ma (2 s.d.). In addition, the measurement of thallium in adularia can be an exploratory guide for nearby ore deposits of base metals.

Based on a detailed revision of the bibliography and the present work, two groups of adularia can be defined, both of which are represented by a feldspar of high potassium composition (~Or₉₀ to Or₁₀₀). The first comprises valencianite s.l. (true valencianite and probably alpine adularia), crystallization of which is controlled by kinetic effects in a hydrothermal environment. Fast growth must be a characteristic parameter that produces various structural states and Al-Si ordering. The second group includes adularia (neofomed K-feldspars) from plutonic, metamorphic, and sedimentary rocks that are more widespread than supposed and deserve more study for their importance in deciphering the fluid and thermal histories of these rocks. This type of adularia grew more peacefully than valencianite and underwent structural changes in later times.

Valencianite can or cannot be a new mineral. Some classical data, new structure refinements, and a recent 'mineral species' definition gave contradictory answers. A solution is not yet attained, but the particular morphological and structural characteristics of valencianite and the misleading application of the term 'mineral variety' to the alkali feldspar minerals need to be included in any discussion about the definition or not of a new mineral species.

Author Contributions: Conceptualization, J.S. and T.P.-P.; methodology, J.S., T.P.-P., and A.O.-R.; software, T.P.-P.; validation, J.S., T.P.-P., and A.O.-R.; formal analysis, J.S., T.P.-P., and A.O.-R.; investigation, J.S., T.P.-P.; resources, J.S., A.O.-R.; data curation, J.S.; writing—original draft preparation, J.S., T.P.-P.; writing—review and editing, J.S., T.P.-P., and A.O.-R. All authors have read and agreed to the published version of the manuscript.

Funding: This research received no external funding.

Data Availability Statement: All data are presented in the published manuscript.

Acknowledgments: The authors acknowledge Patricia Girón for the X-ray fluorescence (XRF) analyses. An anonymous reviewer made interesting comments that improve the manuscript. We truly appreciate the critical and insightful comments from another anonymous reviewer that substantially improved some important parts of the manuscript.

Conflicts of Interest: The authors declare no conflict of interest.

Appendix A

Besides descriptions and geochemical analyses reported from valencianite in the 20th century, there have been very few detailed descriptions of this remarkable mineral. A chronological review of the bibliography dealing mainly with adularia, including sometimes the study of Guanajuato valencianite, follows.

Mallard [63] was the first to describe the optical properties of adularia in his study of anomalous optical phenomena in crystallized substances. He described quickly (p. 320 of the German translation) that a Saint Gotthard (Switzerland) transparent adularia crystal was cut perpendicular to the *c* axis, and four diagonal sectors pointing to the vertex are visible; the opposed showing the same extinction. However, both inclined to the diagonal 2–3°, the two other show the same phenomena, and both optical orientations change in the middle part. Thus, he deduced that adularia shows a complete transition from true monoclinic to homogeneous orthoclase.

Tutton [64] briefly described the structure of adularia from Saint Gotthard, indicating that “adularia consists of a single kind of space-lattice and forms a homogenous solid-solution” based on the stereographic projection of the X-ray diffraction Laue spots.

Spencer [65] made a review of the available published data from adularia. The work deals with the optical and chemical composition of natural and heated specimens. The crystal structure is only briefly reviewed, citing the work of Kôzu and Endô [66], which has already been cited by [64].

Chaisson [48] studied the optics of triclinic adularia from various localities, including valencianite from Guanajuato. After discussing the monoclinic nature of adularia reported in the literature, she described the optical properties of their samples and concluded that these crystals are monoclinic in their cores but deviate to triclinic symmetry towards the surfaces. She observed that adularia has a distinct optical behavior compared to sanidine, orthoclase, and microcline: “As adularia loses its monoclinic symmetry and becomes triclinic, its optical orientation and axial angle vary in the direction of sanidine rather than of microcline.” For this and other reasons, this author proposed that adularia was a real variety of potash feldspar. It is from the structural standpoint that adularia is different from high-K sanidine or orthoclase. She found that valencianite has a $2V_\alpha$ angle of $52\text{--}56^\circ$, and it is neither parallel nor perpendicular to (010).

Laves [67] used the same specimens studied by [48] and determined their structure by X-ray diffraction. For valencianite, the angles were $\alpha = 89^\circ 57'$ and $\gamma = 90^\circ 24'$. He concluded that triclinic adularia is disordered and never ordered due to the low temperature of formation.

Gubser and Laves [61] made a detailed study of 105 specimens of adularia. They try to define adularia based on structural properties (cell dimensions and Al/Si order). It is deduced that adularia can be completely disordered like sanidine, which is not in equilibrium with its formation temperature. A continuous change to the ordered structure is supposed to occur slowly, but they found very few adularia with a completely ordered microcline structure (the final stable state). This work is the only one in this bibliographical review that defines this mineral: “Adularia” is a “mineral” but need not necessarily be a “stable” phase in a thermodynamic sense. From a structural and textural point of view, it may be a “sanidine,” a “microcline,” or an “orthoclase,” or anything intermediate between these states that are (in principle) capable of being rather rigorously defined” ([61], p.187).

Colville and Ribbe [68] presented a detailed study of the structure of the adularia Spencer B from [53]. The structure, refined by least-square methods using 750 reflections, gave monoclinic $C2/m$ symmetry, but the authors emphasize the presence of triclinic domains and weak, diffuse reflections indicating some sort of short-range ordering. These reflections indicate a probable $P21/a$ space group, however these authors preferred to assign it to $C2/m$ to correlate the average Al/Si distribution. Chemical composition is also reported, and the proportion of orthoclase is $\sim 89\%$.

Bass and Ferrara [69] described some adularia from quartz veins in Arkansas dated by Rb–Sr and K–Ar. The structural information (monoclinic vs. triclinic) is given on an informal basis to justify the ages found. It is mentioned here because it is cited by later works on adularia, in which [69] found adularia with diverse ordering states, from highly ordered to highly disordered, and suggest that the ordering increases with time.

Steiner [70] studied an adularia from the Wairakei geothermal field in New Zealand. This adularia precipitated in fissures and replacements from a fluid (hot water and steam) at a maximum of 265°C . The most relevant adularia for our purposes is that found in incrustation on fissured wall rock. It presents the typical {110} faces and is 2.5 mm in size on average. Under optical microscopy, these crystals are defined as homogenous or with patchy extinction or diffuse microcline domains. The structure is described, by X-ray diffraction, as monoclinic, but optical properties also show triclinic domains. The presented diffractogram ([70], his Figure 3) shows some broad peaks, characteristic of feldspars with symmetry variations. The presence of a monoclinic-triclinic mixture is considered primary, but it is postulated that this adularia can also be completely triclinic.

The monoclinic structure is only apparent, simulated by microscopic twinning so that hydrothermal K-feldspars can have any Al/Si ordering on crystallization. The chemical composition is near 100% orthoclase.

Halliday and Mitchell [71] gave a geochronological study of adularia from the Lizard Complex, England, including an X-ray study to distinguish monoclinic vs. triclinic varieties based on the calculation of obliquity. Most crystals were monoclinic with a small proportion of a triclinic phase of variable triclinicity (obliquity). They found a correlation of obliquity and age, indicating that ideal monoclinic adularia preserves the real crystallization age, and the triclinic domains give the age of a low-temperature fluid that replaced parts of the adularia. It is important to note that these authors do not believe that triclinic adularia was either primary or was produced by slow ordering through time. A similar conclusion with K-feldspars from some batholiths in the Catalan Coastal Ranges, NE Spain, was derived by Solé et al. [72] using X-ray diffraction, stable isotopes, and geochronology.

Although not dealing explicitly with Guanajuato adularia, the work of Akizuki and Sunagawa [49] is remarkable in several ways. First, they studied some adularia from Japan and Switzerland and confirmed the findings of Chaisson [48]. Moreover, after a detailed optical study, these authors concluded that the coexistence of monoclinic and triclinic adularia in the same crystal is due to preferential ordering in different faces during crystal growth. Thus, {110} faces are triclinic and disordered, while {001} and {−101} faces are monoclinic and ordered.

Mensing and Faure [18] described 14 samples of K-feldspar extracted from a drill core in the Precambrian basement from Scioto County, Ohio, USA. The work deals with the optical characteristics, chemistry, and age; no X-ray data are presented. The upper five samples were described as adularia that forms overgrowths and cleavage replacements on primary K-feldspars. Based on chemistry and Rb-Sr ages, these authors concluded that the primary feldspars (~1160 Ma) were first converted to clay minerals by late Precambrian weathering and later (~600 Ma or younger), these clays were dissolved by low-temperature hydrothermal fluids and converted to adularia.

Černý and Chapman [73] studied samples of adularia from late hydrothermal veins in pegmatites of diverse localities. They describe these adularia as having a uniform morphology, the Felsöbánya-Maderaner habit (see Figure 3) and a composition near 100% orthoclase. The unit cell dimensions and optical and IR-spectra indicate structural states that range from maximum microcline to high sanidine. Some of the structural states are described as extreme. They discussed the influence of the K/(K+Na) ratio of the solution from which adularia crystallized on its structural state, but the conclusions seem ambiguous.

Borutskiy et al. [74] describe adularia from the Khibiny massif (1481/E) used in our plots. However, no discussion is made about the origin of the adularia.

Černý and Chapman [40] determined the cell parameters of some adularia from hydrothermal deposits, including Guanajuato adularia. They concluded that Al/Si order-disorder in adularia is controlled mainly by the temperature of formation. High temperature gives ordered adularia, and low temperature favors Al/Si disorder. Late fluids seem to have had a significant role in Al/Si order. Many of the studied adularia plots clearly outside the classical *b-c* diagram.

Muszyński and Wyszomirski [75] studied several adularia samples from veins near Zawiercie, Poland. X-ray data, chemistry, infrared (IR), and optical observation were presented, but no structural calculations (cell parameters) were made. The authors observed that small and transparent crystals up to about 2 mm show sector zoning and wavy extinction. In addition, they displayed small optical axial angles under the microscope, from some degrees to a dozen, sometimes up to 40°. The authors used the reflections -201 , 060 , and -204 to deduce that Al/Si ordering is low, at most medium, and structurally resemble high sanidine. Infrared data pointed to the same conclusions. Sodium content was low, $\leq 0.5\%$ Na₂O, and barium could amount to 1%.

Bambauer et al. [14] made a detailed revision of the nomenclature of K-feldspars from two metamorphic sequences in the Alps and Scotland. They made a comparison between

optical, X-ray, and TEM nomenclature. The terms ‘modifications’ and ‘varieties’ are used to describe these differences. Adularia only appears to clarify that the main Figure 7 does not plot it due to its different ordering path.

Ferguson et al. [76] used single-crystal refinement to describe four adularia crystals that gave sanidine-like structures completely disordered. Unlike magmatic sanidines, these crystals were compositionally equivalent to almost pure orthoclase, without appreciable sodium. These crystals refined well in the C2/m spatial group. Three samples showed incipient ordering. Its genesis is like the one described by [39].

Dong and Morrison [77] studied 10 epithermal veins from Queensland, Australia, which furnished four adularia morphologies. Chemistry showed a near pure orthoclase end member. The structural state seemed to be linked to the morphology of crystals (“textural type”), which the authors interpreted as different deposition conditions. Al/Si ordering evolved from high order (sub-rhombic crystals) to median disorder (tabular and rhombic) up to high disorder (pseudo-acicular). Crystallization conditions were slow in the first case to fast in the second and last. Boiling was also indicated in the latter case, producing the disordered structure.

Zhou et al. [78] described the structure of an adularia from Hishikari, Japan. Like all described adularia so far, the chemical composition was almost pure orthoclase. The structure was determined by powder X-ray diffraction, giving a monoclinic highly disordered sanidine. IR and nuclear magnetic resonance (NMR) spectra complemented the study. The authors concluded that this adularia contained triclinic domains, although this deduction was based solely on the NMR spectra, not X-ray diffraction. Rapid crystallization with probable boiling was the preferred crystallization condition.

Bermanec et al. [79] described a remarkable transformation of centimeter-sized adularia to microcline in two pegmatites from Brazil. The authors used X-ray diffraction and TEM to conclude that the crystals that initially had monoclinic structure and adularia morphology had been transformed to completely ordered maximum microcline in solid-state. However, the authors were not sure about the use of the term adularia for these feldspars.

Sánchez-Muñoz et al. [47] made a study of K-feldspars considering order-disorder not only from the point of view of Si/Al tetrahedral cations but also took into account K/Na cavity cations. They analyzed eight adularia samples, including one valencianite from La Valenciana, Mexico. This work presented detailed NMR plus chemical and X-ray diffraction measurements. The authors compared the information obtained with X-ray diffraction with those from NMR and distinguished average and local structures and ordering ranges. They suggested that valencianite must be a new mineral based on triclinicity and a medium-range atomic ordering scheme different from that of sanidine.

Finally, Xu et al. [80] described a new member of the K-feldspar series that they called nano-phase KNA.

References

1. Van der Plas, L. The identification of detrital feldspars. In *Developments in Sedimentology*; Elsevier: Amsterdam, The Netherlands, 1966; Volume 6, 305p.
2. Smith, J.V. *Feldspar Minerals. 1. Crystal Structure and Physical Properties*; Springer-Verlag: Berlin/Heidelberg, Germany, 1974; 627p.
3. Smith, J.V. *Feldspar Minerals. 2. Chemical and Textural Properties*. Springer-Verlag: Berlin/Heidelberg, Germany, 1974; 686p.
4. Ribbe, P.H. *Feldspar Mineralogy*. In *Reviews in Mineralogy*, 2nd ed.; Ribbe, P.H., Ed.; The Mineralogical Society of America: Chantilly, VA, USA, 1975; Volume 2, 362p.
5. Brown, W.L. *Feldspars and Feldspathoids. Structures, Properties and Occurrences*; NATO ASI Series C: Mathematical and Physical Science; Brow, D.L., Ed.; Springer-Science + Business Media: Dordrecht, The Netherlands, 1983; Volume 137, 541p. [[CrossRef](#)]
6. Ribbe, P.H. *Feldspar Mineralogy*. In *Reviews in Mineralogy*, 2nd ed.; Ribbe, P.H., Ed.; The Mineralogical Society of America: Chantilly, VA, USA, 1983; Volume 2, 362p.
7. Smith, J.V.; Brown, W.L. *Feldspar Minerals. Crystal Structures, Physical, Chemical, and Microtextural Properties*; Springer-Verlag: Berlin/Heidelberg, Germany, 1988; Volume 1, 828p.
8. Parsons, I. *Feldspars and Their Reactions*; NATO ASI Series C: Mathematical and Physical Sciences; Parsons, I., Ed.; Springer-Science + Business Media: Dordrecht, The Netherlands, 1993; Volume 421, 650p.
9. Deer, W.A.; Howie, R.A.; Zussman, J. *Rock-Forming Minerals: Framework Silicates: Feldspars*, 2nd ed.; Geological Society of London: London, UK, 2001; Volume 4A.

10. Parsons, I.; Fitz Gerald, J.D.; Heizler, M.T.; Heizler, L.L.; Ivanic, T.; Lee, M.R. Eight-phase alkali feldspars: Low-temperature cryptoperthite, peristerite and multiple replacement reactions in the Klokken intrusion. *Contrib. Mineral. Petrol.* **2013**, *165*, 931–960. [[CrossRef](#)]
11. Martin, R.F. The K-feldspar mineralogy of granites and rhyolites: A generalized case of pseudomorphism of the magmatic phase. *Rendiconti Società Italiana di Mineralogia e Petrologia* **1988**, *43*, 343–354.
12. Lacroix, A. *Minéralogie de Madagascar*; A. Challamel: Paris, France, 1922; Volume 1, pp. 557–562.
13. Blasi, A.; De Pol Blasi, C. Crystal structures of alkali feldspars from granitic pegmatites: A review. *Memorie della Società Italiana di Scienza Naturali e del Museo Civico di Storia Naturale Milano* **2000**, *30*, 73–109.
14. Bambauer, H.U.; Krause, C.; Kroll, H. TEM-investigation of the sanidine/microcline transition across metamorphic zones: The K-feldspar varieties. *Eur. J. Mineral.* **1989**, *1*, 47–58. [[CrossRef](#)]
15. Pini, E. *Memoria Mineralogica sulla Montagna e sui Contorni di S. Gottardo*; Stamperia di Giuseppe Marelli: Milan, Italy, 1783; 128p. + xvi.
16. Eastwood, A.; Oze, C.; Fraser, S.J.; Cole, J.; Gravley, D.; Chambefort, I.; Gordon, K.C. Application of Raman spectroscopy to distinguish adularia and sanidine in drill cuttings from the Ngatamariki Geothermal Field, New Zealand. *New Zealand J. Geol. Geop.* **2015**, *58*, 66–77. [[CrossRef](#)]
17. Kastner, M.; Siever, R. Low temperature feldspar in sedimentary rocks. *Am. J. Sci.* **1979**, *279*, 435–479. [[CrossRef](#)]
18. Mensing, T.; Faure, G. Identification and age of neoformed Paleozoic feldspar (adularia) in Precambrian basement core from Scioto County, Ohio, USA. *Contrib. Mineral. Petrol.* **1983**, *82*, 327–333. [[CrossRef](#)]
19. Duffin, M.E. Nature and origin of authigenic K-feldspar in Precambrian basement rocks of the North American midcontinent. *Geology* **1989**, *17*, 765–768. [[CrossRef](#)]
20. Taylor, P.S. Mineral variations in the silver veins of Guanajuato, Mexico. Ph.D. Thesis, Dartmouth College, Hanover, NH, USA, 1971; 139p.
21. Gross, W.H. New ore discovery and source of silver-gold veins, Guanajuato, Mexico. *Econ. Geol.* **1975**, *70*, 1175–1189. [[CrossRef](#)]
22. Nieto-Samaniego, A.F.; Báez-López, J.A.; Levresse, G.; Alaniz-Álvarez, S.A.; Ortega-Obregón, C.; López-Martínez, M.; Noguez-Alcántara, B.; Solé-Viñas, J. New stratigraphic, geochronological, and structural data from the southern Guanajuato Mining District, México: Implications for the caldera hypothesis. *Int. Geol. Rev.* **2016**, *58*, 246–262. [[CrossRef](#)]
23. Randall, R.J.A.; Saldaña, A.E.; Clark, K.F. Exploration in a volcano-plutonic center at Guanajuato, Mexico. *Econ. Geol.* **1994**, *89*, 1722–1751. [[CrossRef](#)]
24. Moncada, D.; Mutchler, S.; Nieto, A.; Reynolds, T.J.; Rimstidt, J.D.; Bodnar, R.J. Mineral textures and fluid inclusion petrography of the epithermal Ag-Au deposits at Guanajuato, Mexico: Application to exploration. *J. Geochem. Explor.* **2012**, *114*, 20–35. [[CrossRef](#)]
25. Fries, C., Jr.; Hibbard, C.W.; Dunkle, D.H. Early Cenozoic vertebrates in the red conglomerate at Guanajuato, Mexico. *Smithson. Misc. Collect.* **1955**, *123*, 25.
26. Edwards, J.D. Studies of some early Tertiary red conglomerates of central Mexico. *Geol. Surv. Prof. Paper* **1955**, *P0264-H*, 185.
27. Aranda-Gómez, J.J.; Godchaux, M.M.; Aguirre-Díaz, G.J.; Bonnichsen, B.; Martínez-Reyes, J. Three superimposed volcanic arcs in the southern Cordillera—From the Early Cretaceous to the Miocene, Guanajuato, Mexico. In Proceedings of the Geologic Transects Across Cordilleran Mexico, Guidebook for Field Trips of the 99th Annual Meeting of the Cordilleran Section of the Geological Society of America, Mexico City, Mexico, 5–8 April 2003; Publicación Especial 1, Field Trip 6. Universidad Nacional Autónoma de México, Instituto de Geología: Mexico City, Mexico, 2003; pp. 121–168.
28. Godchaux, M.M.; Bonnichsen, B.; Aguirre Diaz, G.; De, J.; Aranda Gomez, J.J.; Rangel Solis, G. Volcanological and tectonic evolution of a complex Oligocene caldera system, Guanajuato mining district, central Mexico. *Geol. Soc. Am.* **2003**, *35*, 8, (Abstracts with Programs).
29. Buchanan, L.J. Ore controls of vertically stacked deposits, Guanajuato, Mexico. *Soc. Min. Eng. Am. Inst. Min. Metall. Pet. Eng.* **1980**, *80–82*, 27.
30. Camprubí, A.; Albinson, T. Epithermal deposits in Mexico—update of current knowledge, and an empirical reclassification. *Geol. S. Am. S.* **2007**, *422*, 377–415. [[CrossRef](#)]
31. Petruck, W.; Owens, D. Some mineralogical characteristics of the silver deposits in the Guanajuato mining district, Mexico. *Econ. Geol.* **1974**, *69*, 1078–1085. [[CrossRef](#)]
32. Moncada, D.; Baker, D.; Bodnar, R.J. Mineral textures and fluid inclusion petrography of the epithermal Ag–Au deposits at Guanajuato, México. *Ore Geol. Rev.* **2017**, *89*, 143–170. [[CrossRef](#)]
33. Del Río, A.M. *Elementos de Orictognosia: Ó del Conocimiento de los Fósiles, Según el Sistema de Berzelio; y Según los Principios de Abraham Góttlob Wérner*; Parte 1; Imprenta de J. F. Hurltel: Filadelfia, PA, USA, 1832; p. 684.
34. Humboldt, A. *Voyage aux Régions Equinoxiales du Nouveau Continent, Fait en 1799, 1800, 1801, 1802, 1803 et 1804, Par Al. De Humboldt et A. Bonpland; Rédigé Par Alexander de Humboldt; Avec un Atlas Géographique et Physique*; Librairie rue git le coeur: Paris, France, 1820; Volume 30, pp. 1805–1834.
35. Rietveld, H. A profile refinement method for nuclear and magnetic structures. *J. Appl. Cryst.* **1969**, *2*, 65–71. [[CrossRef](#)]
36. Cheary, R.W.; Coelho, A.A. A fundamental parameters approach of X-ray line-profile fitting. *J. Appl. Crystallogr.* **1992**, *25*, 109–121. [[CrossRef](#)]

37. Lozano, R.; Bernal, J.P. Characterization of a new set of wight geochemical reference materials for XRF major and trace element analysis. *Rev. Mex. Cienc. Geol.* **2005**, *22*, 329–344.
38. Clark, A.H.; Archibald, D.A.; Lee, A.W.; Farrar, E.; Hodgson, C.J. Laser probe $^{40}\text{Ar}/^{39}\text{Ar}$ ages of early- and late-stage alteration assemblages, Rosario porphyry copper-molybdenum deposit, Collahuasi District, I Region, Chile. *Econ. Geol.* **1988**, *93*, 326–337. [[CrossRef](#)]
39. Goldschmidt, V. *Atlas der Krystallenformen. Band III Danalith-Feldspat-Gruppe*; Carl Winters Universitäts Buchhandlung: Heidelberg, Germany, 1916; Text, 240, 247p.
40. Černý, P.; Chapman, R. Adularia from hydrothermal vein deposits: Extremes on structural state. *Can. Mineral.* **1986**, *24*, 717–728.
41. Franke, W.; Ghobarkar, H. The morphology of hydrothermally grown K-feldspar. *Neues Jb. für Miner. Monat.* **1982**, *2*, 57–68.
42. Woensdregt, C.F. Crystal morphology of monoclinic potassium feldspars. *Z. Kristallogr.* **1982**, *161*, 15–33. [[CrossRef](#)]
43. Kalb, G. Die Kristalltracht des Kalifeldspates in minerogenetischer Betrachtung. *Centr. Min. Abt. A* **1924**, *449–460*, 449–460.
44. Pupin, J.P. Zircon and granite petrology. *Contrib. Mineral. Petrol.* **1980**, *73*, 207–220. [[CrossRef](#)]
45. Evzikova, N.Z. *Prospecting Crystal Morphology*; Nauka: Moscow, Russia, 1984; 144p. (In Russian)
46. Sunagawa, I. *Crystals: Growth, Morphology and Perfection*; Cambridge University Press: Cambridge, UK, 2005; 295p.
47. Sánchez-Muñoz, L.; Sanz, J.; Sobrados, I.; Gan, Z. Medium-range order in disordered K-feldspars by multinuclear NMR. *Am. Mineral.* **2013**, *98*, 2115–2131. [[CrossRef](#)]
48. Chaisson, U. The optics of triclinic adularia. *J. Geol.* **1950**, *58*, 537–547. [[CrossRef](#)]
49. Akizuki, M.; Sunagawa, I. Study of the sector structure in adularia by means of optical microscopy, infra-red absorption, and electron microscopy. *Mineral. Mag.* **1978**, *42*, 453–462. [[CrossRef](#)]
50. Bambauer, H.H.; Laves, F. Zum Adularproblem I. *Schweiz. Miner. Petrog.* **1960**, *40*, 177–205.
51. Hovis, G.L. Determination of chemical composition, state of order, molar volume, and density of a monoclinic alkali feldspar using X-ray diffraction. In *Teaching Mineralogy*; Brady, J.B., Mogk, D.W., Perkins, D., Eds.; Mineralogical Society of America: Washington, DC, USA; Schoell: Paris, France, 1997; pp. 107–118.
52. Wright, T.L.; Stewart, D.B. X-ray and optical study of alkali feldspar: I. Determination of composition and structural state from refined unit-cell parameters and 2V. *Am. Mineral.* **1968**, *53*, 38–87.
53. Spencer, E. The potash-soda feldspars. I. Thermal stability. *Mineral. Mag.* **1937**, *24*, 453–494. [[CrossRef](#)]
54. Sahl, K.; De Albuquerque, C.A.R.; Shaw, D.M. Thallium. In *Handbook of Geochemistry*; Wedepohl, K.H., Ed.; Springer-Verlag: Berlin/Heidelberg, Germany, 1974; Volume II-5, Chap. 81; 60p.
55. Kyono, A.; Kimata, A. The crystal structure of synthetic $\text{TlAlSi}_3\text{O}_8$: Influence of the inert-pair effect of thallium on the feldspar structure. *Eur. J. Mineral.* **2001**, *13*, 849–856. [[CrossRef](#)]
56. Rader, S.T.; Mazdab, F.K.; Barton, M.D. Mineralogical thallium geochemistry and isotope variations from igneous, metamorphic, and metasomatic systems. *Geochim. Cosmochim. Acta* **2018**, *243*, 42–65. [[CrossRef](#)]
57. Martínez-Reyes, J.J.; Camprubí, A.; Tonguç Uysal, I.; Iriondo, A.; González-Partida, E. Geochronology of Mexican mineral deposits. II: Veta Madre and Sierra epithermal vein systems, Guanajuato district. *B. Soc. Geol. Mex.* **2015**, *67*, 349–355. [[CrossRef](#)]
58. Steiger, R.H.; Jäger, E. Subcommittee on geochronology: Convention on the use of decay constants in geo- and cosmochronology. *Earth Planet. Sci. Lett.* **1977**, *36*, 359–362. [[CrossRef](#)]
59. Rotenberg, E.; Davis, D.W.; Amelin, Y.; Ghosh, S.; Bergquist, B.A. Determination of the decay-constant of ^{87}Rb by laboratory accumulation of ^{87}Sr . *Geochim. Cosmochim. Acta* **2012**, *85*, 41–57. [[CrossRef](#)]
60. Povarennykh, A.S. *Crystal Chemical Classification of Minerals*; Springer Science + Business Media: New York, NY, USA, 1972; Volume 1, 458p.
61. Gubser, R.; Laves, F. On x-ray properties of “adularia”, (K, Na) AlSi_3O_8 . *Schweiz. Miner. Petrog.* **1967**, *47*, 177–188.
62. Hawthorne, F.C.; Mills, S.J.; Hatert, F.; Rumsey, M.S. ontology, archetypes and the definition of ‘mineral species’. *Mineral. Mag.* **2021**, *85*, 125–131. [[CrossRef](#)]
63. Mallard, F. Explications des phénomènes optiques anomaux qui présentent un grand nombre de substances cristallisées. *Annales des Mines* **1876**, *10*, 187–240.
64. Tutton, A.E.H. The structure of adularia and moonstone. *Nature* **1921**, *108*, 352–353. [[CrossRef](#)]
65. Spencer, E. A contribution to the study of moonstone from Ceylon and other areas and of the stability relations of the alkali-feldspars. *Mineral. Mag.* **1930**, *22*, 291–367. [[CrossRef](#)]
66. Kôzu, S.; Endô, Y. X-ray analysis of adularia and moonstone, and the influence of temperature on the atomic arrangement of these minerals. *Sci. Rep. Tôhoku Imp. Univ.* **1921**, *1*, 1–17.
67. Laves, F. The lattice and twinning of microcline and other potash feldspars. *J. Geol.* **1950**, *58*, 548–571. [[CrossRef](#)]
68. Colville, A.A.; Ribbe, P.H. The crystal structure of an adularia and a refinement of the structure of orthoclase. *Am. Mineral.* **1968**, *53*, 25–37.
69. Bass, M.N.; Ferrara, G. Age of adularia and metamorphism, Ouachita Mountains, Arkansas. *Am. J. Sci.* **1969**, *267*, 491–498. [[CrossRef](#)]
70. Steiner, A. Genesis of hydrothermal K-feldspar (adularia) in an active geothermal environment at Wairakei, New Zealand. *Mineral. Mag.* **1970**, *37*, 916–922. [[CrossRef](#)]
71. Halliday, A.N.; Mitchell, J.G. Structural, K-Ar and ^{40}Ar - ^{39}Ar age studies of adularia K-feldspars from the Lizard complex, England. *Earth Planet. Sci. Lett.* **1976**, *29*, 227–237. [[CrossRef](#)]

72. Solé, J.; Cosca, M.; Sharp, Z.; Enrique, P. $^{40}\text{Ar}/^{39}\text{Ar}$ geochronology and stable isotope geochemistry of Late-Hercynian intrusions from north-eastern Iberia with implications for argon loss in K-feldspar. *Int. J. Earth Sci.* **2002**, *91*, 865–881. [[CrossRef](#)]
73. Černý, P.; Chapman, R. Paragenesis, chemistry and structural state of adularia from granitic pegmatites. *Bull. Min.* **1984**, *107*, 369–384. [[CrossRef](#)]
74. Borutskiy, B.Y.E.; Organova, N.I.; Marsiy, I.M.; Simonov, M.A.; Zhelezin, Y.E.P. The crystal structures and Si/Al-ordering in adularia and microcline from Khibiny. *Int. Geol. Rev.* **1985**, *27*, 746–753. [[CrossRef](#)]
75. Muszyński, M.; Wyszomirski, P. Adularia from the basement of the Cracow-Silesian monocline near Zawirzie. *Mineralogia Polonica* **1986**, *17*, 43–54, (plus V plates).
76. Ferguson, R.B.; Ball, N.A.; Černý, P. Structure refinement of an adularian end-member high sanidine from the Buck Claim Pegmatite, Bernic Lake, Manitoba. *Can. Mineral.* **1991**, *29*, 543–552.
77. Dong, G.; Morrison, G.W. Adularia in epithermal veins, Queensland: Morphology, structural state and origin. *Miner. Depos.* **1995**, *30*, 11–19. [[CrossRef](#)]
78. Zhou, L.; Guo, J.; Liu, B.; Li, L. Structural state of adularia from Hishikari, Japan. *Chin. Sci. Bull.* **2001**, *46*, 950–953. [[CrossRef](#)]
79. Bermanec, V.; Horvat, M.; Žigovečki Gobac, Ž.; Zebec, V.; Scholz, R.; Škoda, R.; Wegner, R.; Brito Barreto, S.; Dódon, I. Pseudomorphs of low microcline after adularia fourlings from the Alto Da Cabeça (Boqueirão) and Morro Redondo pegmatites, Brazil. *Can. Mineral.* **2012**, *50*, 975–987. [[CrossRef](#)]
80. Xu, H.; Jin, S.; Lee, S.; Hobbs, F.W.C. Nano-phase $\text{KNa}(\text{Si}_6\text{Al}_2)\text{O}_{16}$ in adularia: A new member in the alkali feldspar series with ordered K-Na distribution. *Minerals* **2019**, *9*, 649. [[CrossRef](#)]